

Effect of stress on microstructures of creep-aged 2524 alloy

Li-wei QUAN^{1,2}, Gang ZHAO¹, Ni TIAN¹, Ming-li HUANG²

1. Key Laboratory for Anisotropy and Texture of Materials (Ministry of Education),
Northeastern University, Shenyang 110004, China;

2. School of Resources and Materials, Northeastern University at Qinhuangdao, Qinhuangdao 066004, China

Received 10 July 2012; accepted 5 December 2012

Abstract: Microstructures of creep-aged 2524 (Al–4.3Cu–1.5Mg) aged at 170 °C with various stresses (0, 173 and 250 MPa) were studied on a creep machine. Ageing hardness curves under various stresses were plotted and the corresponding microstructures were characterized by transmission electron microscopy (TEM). The results show that the value of peak hardness is increased, while the time to reach the peak hardness is reduced under an external stress. Meanwhile, the length of *S*(Al₂CuMg) phase is shorter and the number density of *S* phases is larger in the creep-aged alloy. The predominant contribution to the peak hardness can be ascribed to the GPB zones with an elastic stress.

Key words: creep-age; *S* phase; GPB zone; hardness; dislocation; stress orientation effect

1 Introduction

In order to reduce the cost in the manufacture of airplane, age-forming was explored and studied to meet this requirement. It has drawn much attention as it can decrease the manufacturing processes by combining both ageing treatment and the forming process with elastic stress applied to the alloy sheet during the ageing process [1]. This technology has been successfully applied to airplane [2]. The mechanism of age-forming of binary Al–Cu alloy has been investigated [3–7]. And it was found that the elastic stress can induce stress orientation effect on the precipitate in this alloy. However, there are few reports on the age-forming of ternary Al–Cu–Mg alloy. In previous work, the effects of plastic stress on the microstructure and mechanical properties of 2524 alloy were investigated, which can lead to a higher hardness and shorter time to peak hardness. Meanwhile, *S* phases contribute to the peak hardness [8]. In the present study, creep-age forming was employed to study the effect of elastic stress on the microstructures and properties of commercial alloy 2524 during isothermal ageing at 170 °C.

2 Experimental

The chemical composition of the commercial 2524 alloy used in this work is listed in Table 1. The specimens were punched from as-received sheet with 4 mm in thickness. Temperature dependence of yield strength was determined to be 251 MPa at 170 °C using an Instron machine. Then the samples with gage length of 22 mm were aged at 170 °C with a creep machine under various constant stresses. The stresses applied to the alloy were 0, 173 (~70% $\sigma_{0.2}$, $\sigma_{0.2}$ =251 MPa at 170 °C) and 250 MPa (~ $\sigma_{0.2}$). Vickers hardness measurement was carried out with 450SVDTM on the aged specimens under a load of 48 N for dwell time of 20 s. Thin foils were prepared by electro-polishing in a twin-jet Tenupol with a 33% nitric acid solution in methanol operated at –25 °C and 13.8 V. FEI CM20 TEM operated at 200 kV was employed to observe the microstructures.

3 Results and discussion

3.1 Hardness curves

Figure 1 depicts the ageing hardness curves of 2524

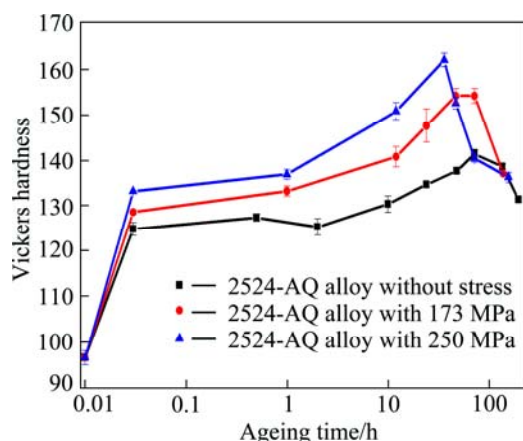
Foundation item: Project (2009BAG12A07-B02) supported by the National Science & Technology Pillar Program during the 11th Five-Year Plan Period, China; Project supported by Innovative Research Team in University of Liaoning Province, China; Project (51001022) supported by the National Natural Science Foundation of China

Corresponding author: Gang ZHAO; Tel: +86-24-83691567; E-mail: zhaog@mail.neu.edu.cn

DOI: 10.1016/S1003-6326(13)62719-3

Table 1 Chemical composition of 2524 commercial alloy (mass fraction, %)

Si	Fe	Cu	Mn	Mg	Cr
0.02	0.1	4.34	0.62	1.45	<0.005
Ni	Zn	Zr	Ti	Al	
<0.005	0.02	<0.005	0.01	Bal.	

**Fig. 1** Hardness curves of creep-aged alloy under various stresses at 170 °C

alloy aged at 170 °C with and without stress during the ageing process. All of the curves are separated into two stages: rapid hardening and second hardening which is consistent with other authors [9–12]. It is generally accepted that the rapid hardening is due to the clusters and the second hardening is ascribed to the GPB zones in this series alloy. When the three groups of samples are shortly aged for 2 min, rapid hardening occurs and the value is increased rapidly compared with the as-quenched condition. Obviously, the hardness value of the creep-aged sample is larger than that of sample conventionally aged at 170 °C. Meanwhile, the hardness value is greater with a larger stress applied to the aged alloy. After leveling for a period, the hardness value begins to ascend the second peak hardness. When applying an external elastic stress on the alloy, the hardness value increases and the time to reach peak hardness decreases compared with the conventional-aged sample. While the peak hardness is much larger and peak time is even shorter under stress of 250 MPa. As for 250 MPa around the yield strength of the alloy responding to the ageing temperature, the increment of the hardness could ascribe to the work hardening effect and the precipitation strengthening. In terms of the alloy under a stress of 173 MPa, the increment of the hardness can be due to the precipitation strengthening. Both will be discussed by associating with microstructures later. In all, the trend of the hardness curves of the alloy applied with elastic stresses is the same with the curves of that under plastic stresses in Ref. [8].

3.2 Microstructures

3.2.1 Microstructural evolution in conventionally aged and creep aged samples

The evolution of the microstructures aged at 170 °C for various time was examined by TEM with the incident beam parallel to $\langle 001 \rangle$ as shown in Fig. 2. A stress of 173 MPa is applied to the alloy to compare the samples without stress. Figure 2(a) shows the typical bright field (BF) TEM image of 2524 alloy aged at 170 °C for 2 min without stress. A few dislocation loops can be observed in this shortly aged sample. However, besides dislocation loops, helical dislocations generate in creep-aged sample aged under 173 MPa for 2 min in Fig. 2(b). The dislocation loops or helical dislocations are on $\{110\}$ plane. The increased dislocations in Fig. 2(b) indicate that the elastic stress can accelerate the formation of dislocations. When the alloy is solution treated and then rapidly quenched, a lot of supersaturated vacancies can be reserved in the matrix. Some dislocation loops can form due to the condensation and collapse of extra vacancies [13]. With an external stress applying on the ageing alloy, the migration of vacancies can be accelerated and the formation of dislocations is facilitated. Thus the number density of dislocations is higher with an external stress applying on the alloy.

With prolonging ageing time to 0.5 h as shown in Fig. 2(c) and Fig. 2(d), it can be seen that the microstructures are similar to those aged for 2 min from the BF TEM images. A few dislocations are present in the conventionally aged alloy and more dislocations are in the creep-aged alloy. Turning to the diffraction pattern, some streaks in both images indicate the presence of the precipitation of $S(\text{Al}_2\text{CuMg})$ phase. However, no other precipitates could be detected in this condition. The precipitate sequence in Al–Cu–Mg alloy which is in the region of $\alpha+S$ phase is generally regarded as: solid solution \rightarrow pre-precipitate stage \rightarrow GPB zones $\rightarrow S \rightarrow S$ [9]. Generally speaking, S phases prefer to nucleate on dislocations and then grow heterogeneously on dislocations. With increasing ageing time, the S phase will grow into lath along $\langle 001 \rangle$ direction on $\{120\}$ plane.

The corresponding microstructures of the ascending stage to peak hardness are shown in Fig. 2(e) and Fig. 2(f). Figure 2(e) illustrates the typical BF TEM image of the 2524 alloy aged at 170 °C for 24 h. S phase can be seen to grow into lath and thicken. While the other strengthening precipitates, GPB zones, could be obviously observed in bright field image and also can be detected in diffraction pattern. Similarly, GPB zones could also be seen in creep-aged sample under a stress of 173 MPa in Fig. 2(f). GPB is nowadays regarded as the predominant precipitates contributing to the peak hardness in the peak-aged Al–Cu–Mg alloy other than

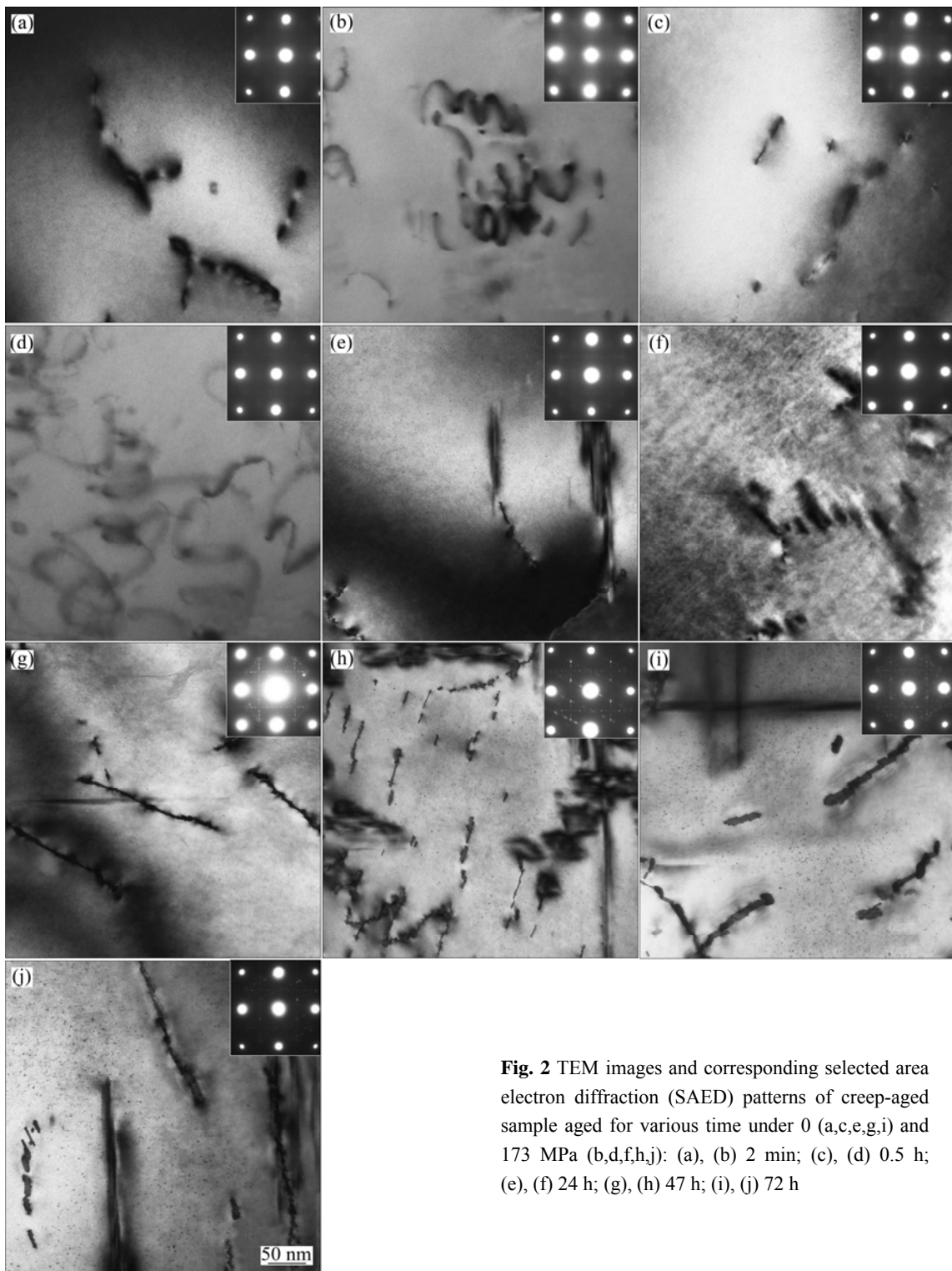


Fig. 2 TEM images and corresponding selected area electron diffraction (SAED) patterns of creep-aged sample aged for various time under 0 (a,c,e,g,i) and 173 MPa (b,d,f,h,j): (a), (b) 2 min; (c), (d) 0.5 h; (e), (f) 24 h; (g), (h) 47 h; (i), (j) 72 h

S phase. And the formation of the GPB zones commences on the end of the plateau of the hardness curves [9]. So, when it is aged for 24 h, GPB zones form homogeneously in the matrix and the hardness increases.

Increasing the ageing time to 47 h, the conventionally aged sample is still in underage condition. The *S* phases grow on dislocations and

distribute equally in each directions in the BF TEM image in Fig. 2(g). This could also be proved by diffraction patterns. The equivalent distribution of the diffraction spots and the intensity indicate the uniform distribution of *S* phases on {210}. Numerous GPB zones uniformly dispersed in the matrix. Similarly, in the creep-aged sample which achieves the peak hardness as illustrated in Fig. 1, the precipitates consist of *S* phase

and GPB zones as shown in Fig. 2(h). Lots of GPB zones could be observed to distribute homogeneously in the matrix. Likewise, the *S* phases distribute equivalently in the creep-aged alloy derived from the diffraction patterns. This means the stress makes no obvious preferential effect on the orientation of *S* phases.

Even for a longer ageing time, in the conventional-aged sample, the microstructures of the peak-age condition are similar as shown in Fig. 2(i). GPB zones are the predominant precipitate and contribute more to the hardness and strengthening. *S* phases coarsely and equivalently distribute in each direction. In the overaged sample under an external stress of 173 MPa (Fig. 2(j)), the number density of GPB zones decreases and the dimensions of GPB zones increase due to Ostwald ripening mechanism compared with the peak-aged sample but the *S* phases still show no preferential orientation. Therefore, it can be obtained that the external stress can accelerate the growth of precipitate to some extent. But the dominant contribution to the peak hardness in the creep-aged alloy under a stress of 173 MPa is ascribed to the GPB zones.

3.2.2 Microstructures of peak-aged sample with various stresses

The microstructures of peak-aged samples at 170 °C with various stresses (0, 173, 250 MPa) are provided in Fig. 3. The *S* phases are in large dimensions with an average length of 414.6 nm and distribute equivalently on all {210} planes as shown in Fig. 3(a). Additionally, the equal distribution can be obtained from the diffraction pattern as well. The intensity of the reflection spots of *S* phases is the same in all directions. It can be clearly seen from Fig. 3(b) that the length of *S* phase is shorter with an elastic stress applied to the alloy. Moreover, larger stress applied to the alloy can induce a remarkably shorter *S* phase as seen in Fig. 3(c). The average length of *S* phase is about 342 nm under 173 MPa and 114.5 nm under 250 MPa. The length of *S* phases is greatly different between Fig. 3(b) and Fig. 3(c). This is because of the number density of dislocations. The smaller dimension of *S* phases could be ascribed to the dislocations which are promoted by external stress. As shown in Fig. 2(b), when applying an external elastic stress to the alloy, the diffusion and the migration of vacancies can be greatly promoted. Dislocations are the favorable channels for vacancies to escape. Thus quantities of dislocations can grow and generate in the matrix. These dislocations provide numerous nucleation sites for the precipitate of *S* phases. Hence, the number density of *S* phases is increased in creep-aged sample. In the later ageing process, the length of *S* phases could not grow larger due to the constant content of solute atoms. Therefore, the length of *S* phases will be shorter but the number density of *S* phases increases in the creep-aged



Fig. 3 TEM images of *S* phases in 2524 alloy aged to peak hardness at 170 °C with various stresses: (a) 0; (b) 173 MPa; (c) 250 MPa

alloy. As for the alloy employed with 250 MPa, the stress is equivalent to the yield strength responding to the ageing temperature, so this can be regarded as a plastic stress. Plastic stress can induce plastic deformation and generate directly more dislocations, which means providing more nucleation sites for the formation of *S* phases. That is why the number density of *S* phases is larger when the alloy is applied with 250 MPa. Meanwhile, the work hardening effect is obvious, so the hardness is high. This is in agreement with other authors

[14,15] and the previous work obtained by the authors with pre-stretching on 2524 alloy [8].

Here it should be noticed that the orientation of S phases does not change even under a stress and they still distribute equally in all directions. This can be also derived from the diffraction patterns which show similar intensity of the spots of S phases. In binary Al–Cu alloy, the preferential orientation of θ' could be observed obviously with a tensile stress or compressive stress [4,16]. It was explained by the misfit between the precipitate and the matrix. θ' has a negative misfit with the matrix and it will nucleate to cancel the misfit to reduce the energy barrier, so the stress can affect the orientation of θ' [2–4]. Also it was assumed that the nucleation of precipitates is primarily affected by external stress. However, it has been known that S phases prefer to heterogeneously nucleate on the dislocations and then grow and coarsen. Lots of dislocations generated in the alloy can give numerous nucleation sites for S phases. The dislocations provide the requisite misfit to cancel the misfit between S phase and matrix. This accommodates the applied stress. So there is no obvious effect of stress on the preferential alignment of S phase. That is why there is no stress orientation effect of precipitates in this kind of alloy.

In terms of the GPB zones, it can be clearly seen that the number density of GPB zones is large in the conventionally aged alloy in Fig. 4(a). And the corresponding SAD pattern in Fig. 4(d) reveals lots of

GPB zones in the alloy. GPB zones are generally considered the predominant precipitate in the peak aged Al–Cu–Mg alloy. And the coarse S phases do not play a great role in the contribution of the peak hardness. Figure 4(a) shows agreement with other authors.

The number of GPB zones is still comparable with the conventionally aged alloy as shown in Fig. 4(b). This could be also seen in Fig. 4(e). However, when increasing the stress to a plastic stress of 250 MPa, the number of GPB zones is sharply decreased in Fig. 4(c). This can be ascribed to the solute atoms attracted to the dislocations to form S phases. When an elastic stress of 173 MPa is applied to the alloy, the dominant contribution to the peak hardness can be due to GPB zones. This is different from the alloys with pre-stretching in which the fine dispersed S phases play a main role in the peak hardness [8]. Plastic stress can induce a large number of dislocations which provide lots of nucleation sites for S phases, while elastic stress can promote the migration of vacancies and solution atoms. Due to the fact that 250 MPa is almost the same with the yield strength at 170 °C, the phenomenon is similar with that in Ref. [8]. This is the difference between elastic stress and plastic stress applied on the alloy. Plastic stress induces many dislocations and leads to very fine S phases, which play a great role in the increase of hardness. However, elastic stress can promote the formation of S phase; the dominant strengthening particles are still GPB zones.

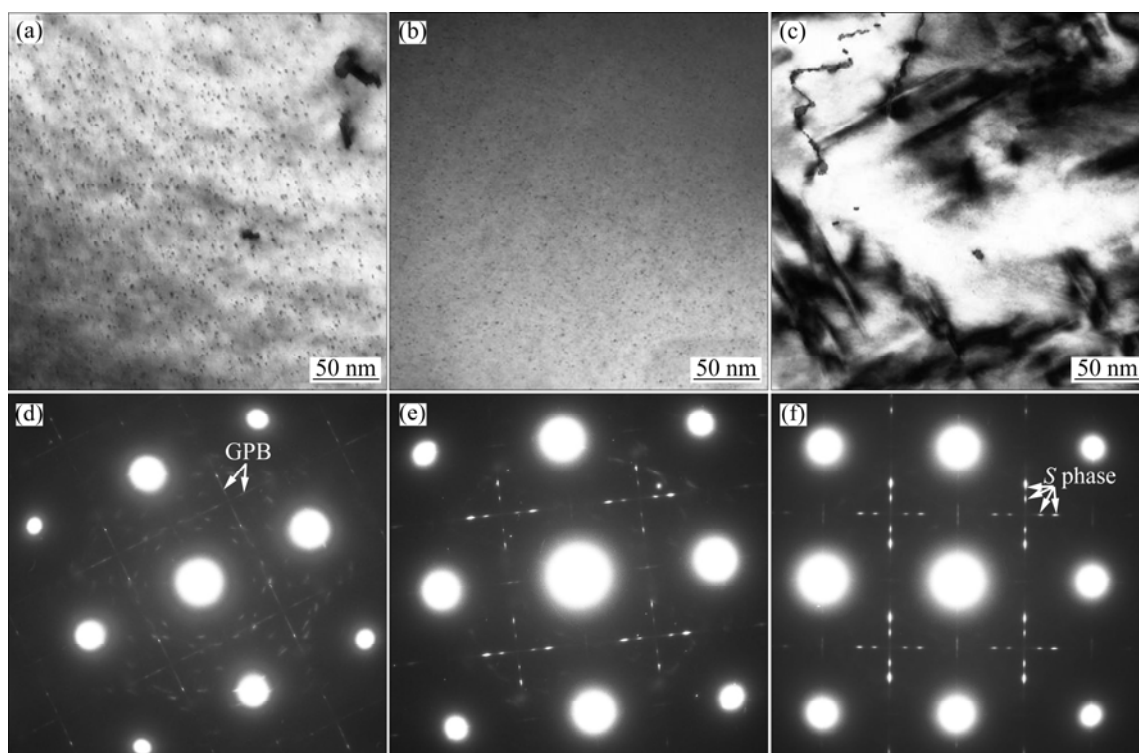


Fig. 4 TEM images (a, b, c) and corresponding SAD patterns (d, e, f) of 2524 alloy aged to peak hardness at 170 °C with various stresses: (a), (d) 0; (b), (e) 173 MPa; (c), (f) 250 MPa

4 Conclusions

1) When an external elastic stress or plastic stress is applying to 2524 alloy, the peak hardness is increased, while the time to reach the peak hardness is reduced.

2) The length of *S* phase is shorter under an external stress and a larger stress can lead to a smaller dimension of *S* phase. Meanwhile, the number density of *S* phase can be facilitated by external stress. However, there is no stress orientation effect on *S* phase of creep-aged alloy.

3) The number density of GPB zones is decreased and only few GPB zones could be observed when the stress is up to 250 MPa approaching to the yield strength.

4) Plastic stress introduces a large number of dislocations providing lots of nucleation sites for *S* phases, while elastic stress promotes the migration of vacancies and solution atoms. GPB zones play a dominant role in the peak-aged sample under a stress of 173 MPa. But *S* phases contribute more to the peak hardness in the creep-aged sample under a stress of 250 MPa.

References

- [1] ADACHI T, KIMURA S, NAGAYAMA T, TAKEHISA H, SHIMANUKI M. Age forming technology for aircraft wing skin [J]. Materials Forum, 2004, 28: 202–207.
- [2] ETO T, SATO A, MORI T. Stress-oriented precipitation for GP zones and θ in an Al–Cu alloy [J]. Acta Materialia, 1978, 26: 499–508.
- [3] SKROTZKI B, SHIFLET G J, STARKE E A Jr. On the effect of stress on nucleation and growth of precipitates in an Al–Cu–Mg–Ag alloy [J]. Metallurgical and Materials Transactions A, 1996, 27: 3431–3444.
- [4] ZHU A W, STARKE E A Jr. Stress aging of Al–xCu alloys: Experiments [J]. Acta Materialia, 2001, 49: 2285–2295.
- [5] BAKAVOS D, PRANGNELL P B, BES B, EBERL F, GARDINER S. Through thickness microstructural gradients in 7475 and 2022 creep-ageformed bend coupons [J]. Materials Science Forum, 2006, 519–521: 407–412.
- [6] ZHU A W, STARKE E A Jr. Stress aging of Al–xCu alloys: Computer modeling [J]. Acta Materialia, 2001, 49: 3063–3069.
- [7] ZHU A W, STARKE E A Jr. Materials aspects of age-forming of Al–xCu alloy [J]. Journal of Materials Processing Technology, 2001, 117: 354–358.
- [8] QUAN Li-wei, ZHAO Gang, GAO Sam, MUBBLE Barry C. Effect of pre-stretching on microstructure of aged 2524 aluminium alloy [J]. Transactions of Nonferrous Metals Society of China, 2011, 21(9): 1957–1962.
- [9] RINGER S P, HONO K, POLMEAR I J, SAKURAI T. Nucleation of precipitates in aged Al–Cu–Mg–(Ag) alloys with high Cu:Mg ratios [J]. Acta Materialia, 1996, 44(5): 1883–1898.
- [10] RINGER S P, HONO K, SAKURAI T, POLMEAR I J. Cluster hardening in an aged Al–Cu–Mg alloy [J]. Scripta Materialia, 1997, 36(5): 517–521.
- [11] RINGER S P, SOFYAN B T, PRASAD K S, QUAN G C. Precipitation reactions in Al–4.0Cu–0.3Mg (wt.%) alloy [J]. Acta Materialia, 2008, 56: 2147–2160.
- [12] RINGER S P, SAKURAI T, POLMEAR I J. Origins of hardening in aged Al–Cu–Mg–(Ag) alloys [J]. Acta Materialia, 1997, 45(9): 3731–3744.
- [13] WESTMACOTDT K H, HULL D, BARNES R S. Dislocation sources in quenched aluminium-based alloys [J]. Philosophical Magazine, 1959, 4 (45): 1089–1092.
- [14] ZHANG Xin-ming, LIU Ling, JIA Yu-zhen. Microstructures and mechanical properties of 2519A aluminum alloy [J]. The Chinese Journal of Nonferrous Metals, 2010, 20(6): 1088–1094. (in Chinese)
- [15] LI Hui-zhong, ZHANG Xin-ming, CHEN Min-gan, ZHOU Zhuo-ping, GONG Min-ru. Effect of pre-deformation on microstructures and mechanical properties of 2519 aluminum alloy [J]. The Chinese Journal of Nonferrous Metals, 2004, 14(12): 1990–1994. (in Chinese)
- [16] HOSFORD W F, AGRAWAL S P. Effect of stress during aging on the precipitation of θ' in Al–4WtPctCu [J]. Metallurgical Transactions A, 1975, 6: 487–491.

应力对蠕变时效 2524 合金微观组织的影响

权力伟^{1,2}, 赵刚¹, 田妮¹, 黄明丽²

1. 东北大学 材料各向异性与织构教育部重点实验室, 沈阳 110004;

2. 东北大学秦皇岛分校 资源与材料学院, 秦皇岛 066004

摘要: 研究了 2524 合金(Al–4.3Cu–1.5Mg)通过蠕变机器施加不同应力(0、173 和 250 MPa)在 170 °C 时效的微观组织变化, 测定了不同应力下的硬度曲线, 并利用透射电镜(TEM)观察相应的微观组织。结果表明: 施加应力的样品, 时效后其峰值硬度增加, 而达到峰值硬度所需的时间缩短; 时效成形后, *S*(Al₂CuMg)相长度变短, 而密度增加; 弹性应力下 GPB 区对峰值硬度起主要作用。

关键词: 蠕变时效; *S* 相; GPB 区; 硬度; 位错; 应力位向效应

(Edited by Hua YANG)